Food Chemistry 197 (2016) 257–265

Contents lists available at ScienceDirect

Food Chemistry

journal homepage: www.elsevier.com/locate/foodchem

Analytical Methods

Prediction of total volatile basic nitrogen contents using wavelet features from visible/near-infrared hyperspectral images of prawn (*Metapenaeus ensis*)

Qiong Dai [a], Jun-Hu Cheng [a], Da-Wen Sun [a,b,*], Zhiwei Zhu [a], Hongbin Pu [a]

[a] College of Light Industry and Food Sciences, South China University of Technology, Guangzhou 510641, China
[b] Food Refrigeration and Computerized Food Technology, Agriculture and Food Science Centre, University College Dublin, National University of Ireland, Belfield, Dublin 4, Ireland

ARTICLE INFO

Article history:
Received 14 July 2014
Received in revised form 7 October 2015
Accepted 18 October 2015
Available online 19 October 2015

Keywords:
Prawn
Hyperspectral image
Wavelet analysis
Total volatile basic nitrogen
TVB-N

ABSTRACT

A visible/near-infrared hyperspectral imaging (HSI) system (400–1000 nm) coupled with wavelet analysis was used to determine the total volatile basic nitrogen (TVB-N) contents of prawns during cold storage. Spectral information was denoised by conducting wavelet analysis and uninformative variable elimination (UVE) algorithm, and then three wavelet features (energy, entropy and modulus maxima) were extracted. Quantitative models were established between the wavelet features and the reference TVB-N contents by using three regression algorithms. As a result, the LS-SVM model with modulus maxima features was considered as the best model for determining the TVB-N contents of prawns, with an excellent R_P^2 of 0.9547, RMSEP = 0.7213 mg N/100 g and RPD = 4.799. Finally, an image processing algorithm was developed for generating a TVB-N distribution map. This study demonstrated the possibility of applying the HSI imaging system in combination with wavelet analysis to the monitoring of TVB-N values in prawns.

1. Introduction

Freshness is a measure of quality in seafood, which deteriorates rapidly after harvesting. Therefore techniques such as refrigeration (Kiani and Sun, 2011; Sun and Eames, 1996; Wang and Sun, 2002a, 2004; Zheng and Sun, 2004) and drying (Cui, Sun, Chen, and Sun, 2008; Delgado and Sun, 2002) are often used to maintain seafood quality. The freshness of seafood is affected by the decomposition of protein, carbohydrates and fat, and the catalysis of enzymes, as well as the metabolism of microorganisms. In order to evaluate the freshness level of seafood products, a variety of methods based on different perspectives, including sensory evaluation (Alasalvar et al., 2001), microbial inspection (Koutsoumanis & Nychas, 2000), biochemical methods (Olafsdottir et al., 1997), chemical volatile compound measurement (Iglesias et al., 2009), protein property determination (Reddy & Srikar, 1991), and proteome analysis (Martinez & Jakobsen Friis, 2004) have been applied. Total volatile basic nitrogen (TVB-N) is regarded as the most effective technique for freshness evaluation (Arvanitoyannis & Stratakos, 2012; Castro, Padrón, Cansino, Velázquez, & Larriva, 2006). In addition, cold storage is the most common storage method, which prolongs the shelf-life of prawns during transport and marketing. Therefore, it might be valuable to determine the variation of TVB-N in prawn during cold storage.

Traditional techniques for determination of TVB-N are laborious, destructive and tedious, which limit their applications for on-line freshness monitoring and control. To overcome these problems, several non-destructive techniques such as spectroscopy, computer vision, and hyperspectral imaging technique have been proposed for measurement of TVB-N. By integrating the advantages of spectroscopy and computer vision (Costa et al., 2011; Jackman, Sun, Du, and Allen, 2009; Sun, 2004; Wang and Sun, 2002b), hyperspectral imaging (HSI) is able to predict the quality attributes at each pixel of the image (Barbin, ElMasry, Sun, and Allen, 2012a,b; ElMasry, Barbin, Sun, and Allen, 2012; ElMasry, Kamruzzaman, Sun, and Allen, 2012; Kamruzzaman, ElMasry, Sun, and Allen, 2012; Lorente et al., 2012; Wu, Sun, and He, 2012; Wu and Sun, 2013). Recently, numerous studies demonstrated that HSI shows the possibility for estimating the chemical composition contents such as fat (Zhu, Zhang, Shao, He, & Ngadi, 2013) and moisture (He, Wu, & Sun, 2013), microbiological attributes such as freshness (Khojastehnazhand et al., 2014) and

* Corresponding author at: Food Refrigeration and Computerized Food Technology, Agriculture and Food Science Centre, University College Dublin, National University of Ireland, Belfield, Dublin 4, Ireland.
E-mail address: dawen.sun@ucd.ie (D.-W. Sun).
URLs: http://www.ucd.ie/refrig, http://www.ucd.ie/sun (D.-W. Sun).

http://dx.doi.org/10.1016/j.foodchem.2015.10.073
0308-8146/

spoilage (Wu & Sun, 2013), as well as sensory parameters such as color (Wu et al., 2012) and texture (Dai, Cheng, Sun, & Zeng, 2014) of fish and other seafoods. In particular, for the determination of TVB-N, Cheng, Sun, Zeng, and Pu (2014) investigated the potential of using HSI system within the spectral wavelength range of 400–1000 nm to determine the TVB-N in grass carp fillets during frozen storage. The range of TVB-N in measured fish fillets was 7.83–16.48 mg N/100 g, which was too narrow to establish a robust prediction model for determining a large variance of TVB-N. In addition, Huang, Zhao, Chen, and Zhang (2014) attempted to measure TVB-N in pork meat by integrating near infrared spectroscopy, computer vision, and the electronic nose technique. However, in the fusion model, the large volume of 83 features adapted from NIRS, CV and E-nose greatly increased the complexity and calculation load of the model (Huang et al., 2014). More importantly, the data mining methods in the above studies used the most traditional and typical algorithms. Therefore, it is important to develop or introduce novel methods to analyze the hyperspectral dataset or signal of seafoods.

The main objective of signal analysis is to find the relationship between time information and frequency information (Allen & Mills, 2004). The transformation of signal from time domain to frequency domain is meaningful for the signal analysis when the frequency components contain some significant features as in the case of hyperspectral images. Due to the transient nature of hyperspectral images produced by food samples, traditional methods such as Fourier transform or short-time Fourier transform are unable to process such signals effectively since the time information is severely reduced after transformation (Boashash, 1991; Grafakos, 2008). Unlike Fourier transform, wavelet transform can obtain both the time and frequency information of a signal simultaneously by shifting a stretched or compressed versions (scale) of wavelet function (mother wavelet) at different locations along the signal. The resulting coefficients generated by different parts of the signal at different scaling factor are called wavelet coefficients. The coefficients resulting from a large scaling factor represent the low frequency components of the signal (approximate value) while those generated by a small scaling factor represent the high frequency components of the signal (detailed value) (Torrence & Compo, 1998). Moreover, signal can be decomposed by several (generally $\leqslant 8$) levels, and for simplicity, further decomposition is only conducted on the approximate value at each decomposition level. Thus, with the decomposition level of n, the spectral features of hyperspectral images can be broken into n high frequency components and 1 low frequency components after 1 dimensional wavelet analysis. Recently, wavelet transform has been recognized as a valuable tool for signal processing (such as noise removal, compression, feature extraction, and reconstruction) of hyperspectral images at multiple resolutions (Abramovich, Bailey, & Sapatinas, 2000). However, little information is available for its application in HSI analysis of foods including seafoods such as prawn. Therefore, the objective of this study was to use wavelet transform and analysis as an effective data mining technique to handle the hyperspectral images of prawns, in order to develop a simple, robust and accurate model for predicting the variation of TVB-N contents in prawn during cold storage.

2. Materials and methods

2.1. Preparation of prawn samples

A total of 240 live prawns (*Metapenaeus ensis*) each weighing approximately 8–10 g were purchased from a local aquatic products market of Xinzhao (Guangzhou, China). The prawns were kept in seawater to which oxygen was added constantly using an oxygen machine during transport to the laboratories of South China University of Technology. After excluding the dead and injured individuals, the remaining prawns were treated with crushed ice (0 °C for 5 min) to induce a sudden death, and peeled immediately by hand. Then the peeled prawns were drained, and packaged in plastic bags, and 240 prawns were divided into five groups (each group having 48 prawns) and stored at 4 °C for 0 h (first group), 24 h (second group), 48 h (third group), 72 h (fourth group) and 96 h (fifth group), respectively. For each cold storage period, prawns were scanned by a HSI system firstly and then their corresponding reference values of TVB-N were determined by traditional methods. The key steps of the experimental procedure are illustrated in Fig. 1.

2.2. Determination of TVB-N

A modified stream distillation method was conducted to measure the reference TVB-N values (Cai, Chen, Wan, & Zhao, 2011). To reduce the effect of muscle composition on cold storage, 3 g of the middle prawn muscle (the second to fifth segments) was minced and then mixed with 27 mL of perchloric acid (0.6 M). After 10 min of reaction, the mixture was centrifuged at 5000 rpm for 10 min, and then 30 mL of 30% sodium hydroxide was added to make the filtrate alkaline and distilled for 5 min using a 8100 Kjeltec Distillation Unit (FOSS Tecator, Hillerød, Denmark). The distillate was collected in a conical flask containing 50 mL aqueous solution of boric acid (40 g/L) and a mixed indicator. Afterward, a 0.01 M of hydrochloric acid solution was used to titrate the obtained boric acid solution, of which the consumption was used to calculate the TVB-N contents (mg N/100 g) in prawn muscle.

2.3. Hyperspectral imaging system and image acquisition

A typical pushbroom HSI system in the spectral range of 308–1105 nm (501 bands) with 1004×1002 pixels, described previously by Dai et al. (2014), was applied to obtain the hyperspectral images of prawn in reflectance mode. Before scanning, the surface moisture of prawns were wiped by paper towel and warmed to room temperature (25 °C). The prawns were then placed on the translation platform and moved to the field of view of the camera at a constant speed of 1.5 mm/s. Thus, a total of 240 hyperspectral images were obtained over the whole cold storage, in which 75% of hyperspectral images were used as the calibration set and the remaining 25% of hyperspectral images formed the prediction set in each cold storage period. As a result, the total size of calibration set and prediction set is 180 and 60, respectively.

By checking the acquired hyperspectral images, a high level of noise was observed at both ends of the working spectral range (308–1105 nm), thus only the spectral range of 400–1000 nm was used for spectral data extraction. Additionally, in order to minimize the effects of illumination and detector sensitivity as well as the differences in camera and physical configuration of the imaging system, a calibration step was conducted with two extra images, namely the black image and the white reflectance image. The black image (~0% reflectance) was acquired by covering the camera lens with its opaque cap while the white reflectance image was obtained using a uniform Teflon white tile (~99% reflectance). The calibration was performed using the following formula:

$$R_c = \frac{R_0 - R_B}{R_W - R_B} \times 100\% \quad (1)$$

where R_0 is the original acquired hyperspectral images, R_B is the standard black reference images, R_W is the standard white reference images and R_C is the calibrated images.

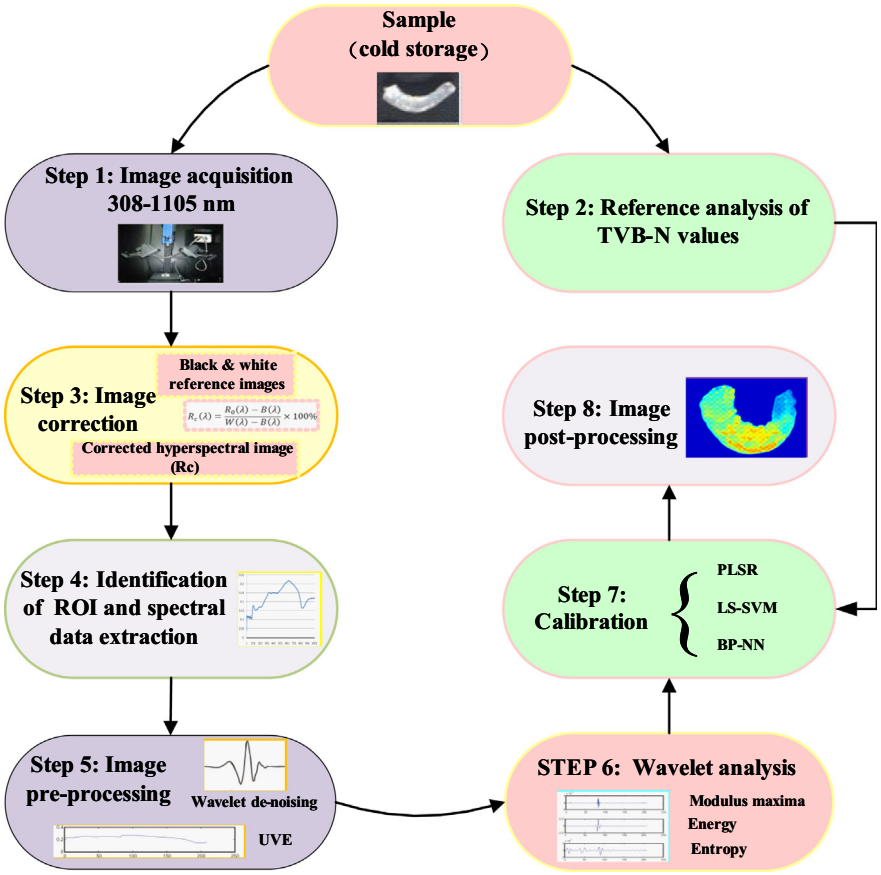

Fig. 1. The key steps of experimental procedure.

2.4. Data pre-treatments

2.4.1. ROI identification and spectra extraction

In order to ensure the corresponding relationship between spectra and reference values, the spectra should be acquired in the areas that were used for reference measurement (Feng & Sun, 2012). In this study, the locations within hyperspectral images, corresponding to areas of prawns that were used for determining the reference TVB-N contents, were recognized as the region of interest (ROI). For consideration of reducing the spatial noise, the averaged spectra were extracted from the ROI of the hyperspectral images by using the procedure of Statistics Average in ENVI v4.8 (ITT Visual Information Solutions, Boulder, CO, USA).

2.4.2. Wavelength reduction

The hyperspectral images obtained were composed of hundreds of contiguous wavelengths for each pixel of a prawn sample, in which most of wavelengths were redundant or weakly related to the final prediction. These useless variables increased the calculation load and were removed in order to generate more accurate and robust classification or predictive models. Several approaches have been demonstrated to be efficient in the eliminating the noise and less important wavelengths by dimension reduction. One of the approaches is to use uninformative variable elimination (UVE), which reduces the number of uninformative wavelengths (Liu, Sun, & Zeng, 2014). In the UVE approach, a PLS regression model should be established, the reliability (an evaluation criterion of importance) of each wavelength is then analyzed based on the corresponding regression coefficients of the PLS regression model (Centner et al., 1996). Then by setting a cut-off value (threshold), the wavelength with reliability higher than the threshold is retained, and the lower ones removed. In this study, the cut-off value (threshold) was set at the absolute stability value of the 99% sorted index number.

2.4.3. Wavelet analysis

The undesired variations, resulting from the physical, environmental or instrumental changes during the procedure of data collection, may decrease the robustness and accuracy of prediction or classification model (Pu, Sun, Ma, Liu, and Cheng, 2014; Pu, Xie, Sun, Kamruzzaman, and Ma, 2015). Thus, pre-treatment for minimizing the undesired variations is required to prepare the data for further analysis. Recently, wavelet transform have been successfully applied in the separation of overlapping bands, noise removal, smoothing, base line correction, and in removing multicollinearity effect of multi-dimensional spectra (Barclay, Bonner, & Hamilton, 1997; Gributs & Burns, 2006). The Daubechies one-dimensional discrete wavelet transform was conducted to analyse the spectra matrix of prawns in this study. A combination of low and high-pass wavelet filters was used to obtain discrete wavelet coefficients of the spectral set (Mallat, 1989). As shown in Fig. 2, the one-dimensional wavelet decomposition at the first level gives two curves comprising of approximate signal (A_1) and detailed signal (D_1). And then the signal length is reduced to half in each filtering operation. In other words, the approximated signal, which is now half-sized compared to the original signal, is further decomposed into the second level of approximated (A_2) and detailed signals (D_2). This process can be repeated until a desired or predefined level is reached. The decomposition levels of spectra matrix in this study was 7.

For de-noising, a wavelet de-noising scheme based on soft and hard thresholding (Donoho, 1995) was employed to remove the

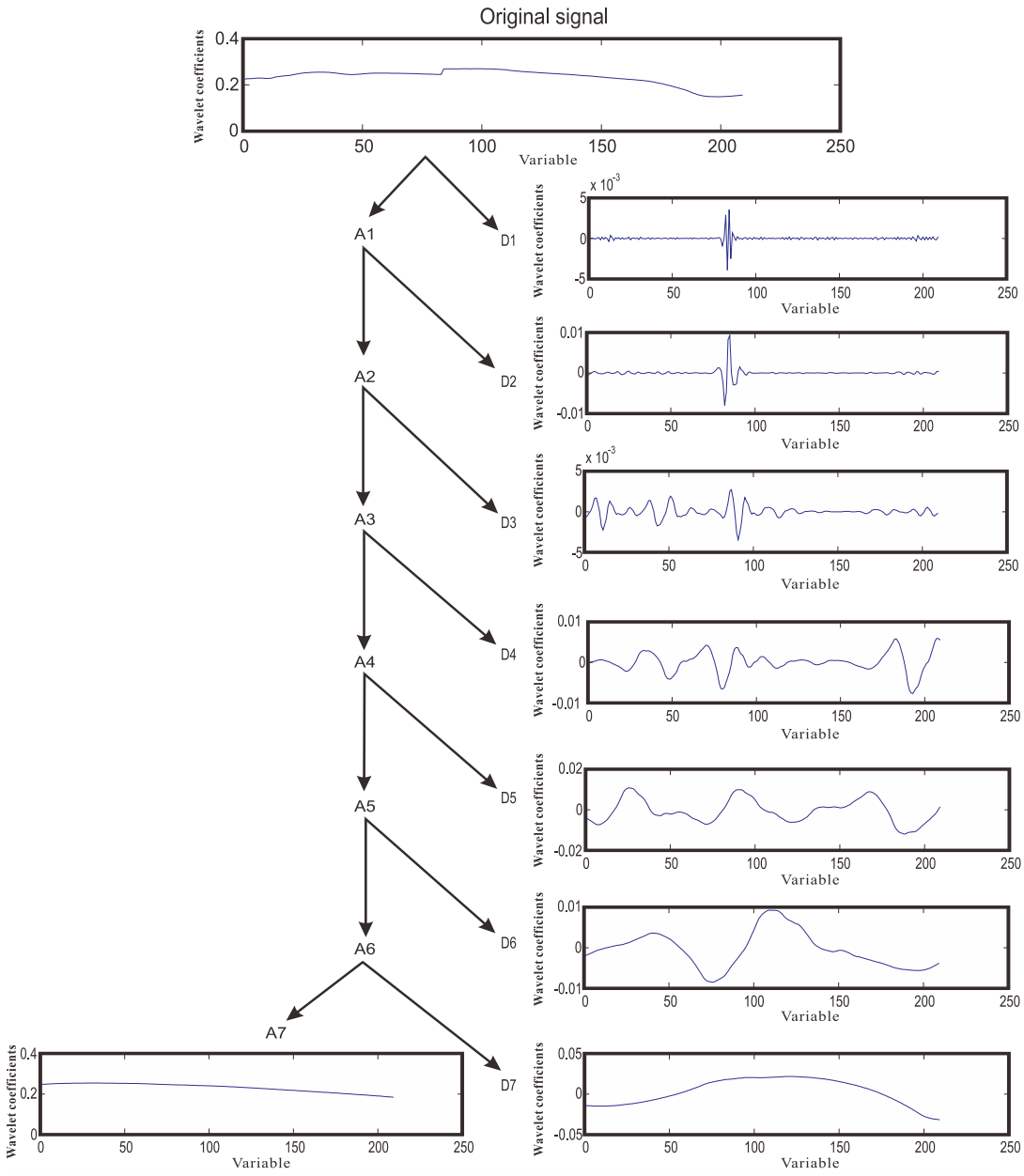

Fig. 2. The wavelet decomposition of a UVE pretreated spectrum (206 wavelengths), centering at 530–660 nm and 780–980 nm.

noise in this study. The main steps are as follows. Assuming that $p(t)$ is the noise-free signal and $f(t)$ is the signal corrupted with white noise $e(t)$, i.e.,

$$f(t) = p(t) + \psi_n e(t) \tag{2}$$

where $e(t)$ obeys a normal distribution $N(0;1)$ and ψ_n is the noise variance.

(1) Convert the continuous signal $f(t)$ to discrete signal $f(i)$ by using uniform sampling.
(2) The signal $f(i)$ is transformed to an orthogonal domain by the usage of discrete wavelet transform.
(3) A soft or hard thresholding is applied to the resulted wavelet coefficients by the following formulae:

$$\text{Soft thresholding function}: s_\gamma(x) = sign(x) \times \max(|x| - \gamma, 0) \tag{3}$$

$$\text{Hard thresholding function}: \begin{matrix} h_\gamma(x) = x \times 1\{|x| > \gamma\} \\ otherwise, h_\gamma(x) = 0 \end{matrix} \tag{4}$$

In Eqs. (3) and (4), γ is defined as:

$$\gamma = \sqrt{2\psi_n^2 \log n} \tag{5}$$

where n is the length of the noisy signal $f(i)$.

(1) The inverse discrete wavelet transform is performed to reconstruct the de-noised signal.

The above de-noising algorithm performs well under a number of applications (Chen, Zhu, & Xie, 2012; Cho, Bui, & Chen, 2009) because wavelet transform is done only on the detailed coefficients (noise) while the approximate coefficients are well retained. In this study, Daubechies wavelet analysis, integrating the advantages of

smoothness and adaptation, was applied to eliminate the undesired variations from the data matrix prior to data modeling.

As for the feature extraction of hyperspectral images, three wavelet features, including energy, entropy signatures, and modulus maxima, were calculated from the resulting wavelet coefficients using the following equations:

$$\text{Energy} = \frac{1}{M_l}\sum_{k_l=1_l}^{M_l}|W_{2^l}[f(t)]|^2 \quad (6)$$

$$\text{Entropy} = -\frac{1}{M_l}\sum_{k_l=1_l}^{M_l}|W_{2^l}[f(t)]|^2 \log|W_{2^l}[f(t)]|^2 \quad (7)$$

The modulus maxima $Max|W_{2^l}[f(t_{k_l})]$ should satisfy the following equation:

$$\begin{cases} |W_{2^l}[f(t)]| > |W_{2^l}[f(t+1)]| \\ |W_{2^l}[f(t)]| > |W_{2^l}[f(t-1)]| \end{cases} \quad l = 1,2,\ldots,L,\ k_l = 1_l, 2_l, \ldots, M_l \quad (8)$$

where l is the scale, k is the number of modulus maxima at scale l, $W_{2^l}[f(t)]$ is the wavelet coefficients of $f(t)$ at the scale of l.

The extraction of wavelet features was achieved by a developed program operated in Matlab 2011a (The MathWorks Inc., Natick, MA, USA) for wavelet analysis. The extracted wavelet features were then used to establish prediction models.

2.5. Model calibration and estimation

The final goal of developing a HSI system is to estimate or discriminate the characteristics of new samples accurately based on the established quantitative models. In order to find the real relationship between TVB-N value and wavelet features, one linear regression method, i.e., partial least squares regression (PLSR) and two non-linear regression methods, i.e., least squares support vector machines (LS-SVM), and back-propagation neural network (BP-NN), were applied to build quantitative calibration models in this study. The performance of the three established models based upon PLSR, LS-SVM, and BR-NN using the wavelet features were compared according to their predicting abilities. Several statistic parameters are available to evaluate the prediction ability, including the determination coefficients (R^2), root mean square error (RMSE), and ratio of prediction to deviation (RPD). Generally, a good model should have a high R^2 and a low RMSE. By combining the ratio of SD and RMSE, RPD presents a relative predictive performance of the established model more directly and efficient than when either R^2 or RMSE is used separately. According to Barlocco, Vadell, Ballesteros, Galietta, and Cozzolin (2006) and Guy, Prache, Thomas, Bauchart, and Andueza (2011), the value of RPD above 2 indicate a good performance of the calibration model, while a RPD value greater than 3 is considered sufficient for a particular analytical purposes. In this study, rather than calculating the ordinary statistical criteria from the established calibration or validation models, the quality of regression models was primarily evaluated by the above three statistics in the prediction set (ElMasry, Sun, & Allen, 2013).

2.6. Visualization

As TVB-N is a comprehensive freshness index that is related to activities such as the degradation of proteins caused by enzymatic and microbial activity, the TVB-N value may vary from pixel to pixel. Therefore, visualization of TVB-N distribution is helpful to understand the overall freshness level of prawns at different cold storage periods. However, it is practically impossible to obtain the reference contents of TVB-N at each pixel of prawn. As a useful imaging tool, HSI is capable of visualizing the spatial distribution of chemical components by generating the images or maps of concentration gradients. In this study, the wavelet features of each pixel was inserted into the optimized calibration model to obtain its corresponding TVB-N content. Then a visualized distribution map was generated by pseudo-coloring each pixel into different colors according to their corresponding TVB-N concentration, which facilitated a better adjudication of the distribution and variations of TVB-N content by checking the different color distributions. All the procedures of visualization were conducted in a developed program using software Matlab 2011a.

3. Results and discussion

3.1. Reference measurement of TVB-N

The reference average TVB-N contents of measured prawns at each cold storage period (Fig. 3) reveal a low average TVB-N value of 13.4 mg N/100 g in the 0 h group, indicating superior freshness. The TVB-N contents were subsequently increased significantly at the storage period of 24 h and 48 h possibly caused by the microbial decomposition of protein. As for the two longer cold storage periods (72 h and 96 h), the TVB-N contents gradually accumulated at a relatively slow rate as the metabolism of protein was effectively restrained (Huang et al., 2014). The TVB-N contents for some samples even exceeded 30 mg N/100 g, which should be rejected for human consumption (Castro et al., 2006; Olafsdottir et al., 1997). The mean, standard deviation (SD) and the range of TVB-N contents measured by the conventional methods in calibration set are 20.75 mg N/100 g, 5.30 mg N/100 g, 9.41–35.40 mg N/100 g and those for the prediction set are 20.23 mg N/100 g, 5.12 mg N/100 g, 9.87–33.52 mg N/100 g. The average TVB-N value of all groups was 20.49 mg/100 g, indicating most of the cold storage ($\leqslant$96 h) samples were acceptable for human consumption (Castro et al., 2006; Olafsdottir et al., 2006). More importantly, the variation of TVB-N contents found in the examined prawn samples, ranging from 9.41 mg N/100 g to 35.4 mg N/100 g, was required for establishing a robust and accurate calibration model. Compared to the prediction set, the larger range in calibration set might be meaningful for improving the prediction accuracy.

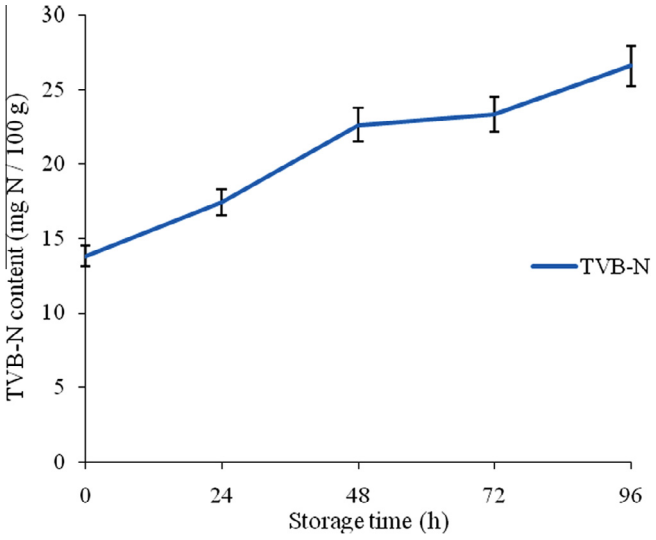

Fig. 3. The variation of TVB-N contents in prawns during cold storage.

3.2. Spectral characteristics

The averaged reflectance spectra of prawns at different cold storage periods within the wavelength range of 400–1000 nm are shown in Fig. 4. A similar trend with some variation was found among the five average reflectance spectra. These differences were possibly attributed to the changes of the main chemical components during the cold storage of prawns. Although different TVB-N values were found between the 0 h group and 24 h group, little difference was observed in the corresponding reflectance spectra. When the cold storage time reached 48 h, the main chemical components of prawns were gradually decomposed, resulting in the rapid accumulation of TVB-N as well as the increases of reflectance values. The increased trend in the first three periods was consistent with Cheng et al. (2013) who identified a positive relationship between the reflectance value and TVB-N contents ($7 < \text{TVB-N} < 16$ mg N/100 g). As most protein had been decomposed in 72 h and 96 h periods, the accumulation of the TVB-N contents were slow and their corresponding decomposition products such as ammonia, hydrogen sulfide, ethyl mercaptan, hydrocarbons, alcohols, ketones and aldehydes accounted for the main factor of spectra absorption, resulting in a declining trend of reflectance spectrum. By checking the reflectance spectra, three broad peeks centered at 575 nm, 810 nm and 970 nm were easily identified. In detail, 575 nm was the feature wavelength for detecting metmyoglobin (Wu et al., 2012), the high reflectance values at 810 nm were possibly due to the combined influences of C–H stretching overtone in protein contents and O–H stretching overtone in water (He et al., 2013; Wu, He, & Feng, 2008), and the peak around 970 nm was mainly related to the second overtone O–H stretching in water as water is the major composition in prawn (Elmasry, Sun, & Allen, 2011; Talens et al., 2013).

3.3. Identification of important wavelengths and extraction of wavelet features

The redundant and noisy wavelengths in the spectral dataset not only decrease the prediction ability but also limit the implementation of HSI for on-line systems. Therefore, it is desirable to conduct wavelength elimination to establish simplified calibration models with higher predicting accuracies. In this study, UVE was employed to reduce the useless wavelengths, aiming to reducing the calculation burden for further analysis. After the application of the UVE algorithm, about 206 wavelengths were selected distributed mainly on two broad regions around 530–660 nm and 780–980 nm, which was consistent with the previous analysis of spectral characteristics. This meant that most of wavelengths in these two regions contained important information for the determination of TVB-N values in prawns during cold storage. Once the redundant wavelengths were removed, three wavelet features, including energy, entropy and modulus maxima were extracted at the identified important wavelength regions. With seven wavelet decomposition levels, eight, eight and twenty variables, respectively, were obtained for energy, entropy and modulus maxima in each sample. In order to find the most appropriate wavelet features for predicting the examined TVB-N contents of prawns, the extracted three wavelet feature sets were used as the input variables for calibration models and their corresponding performance for determining TVB-N contents in the test samples were compared.

3.4. Prediction of TVB-N values based on wavelet features

As the successful implementation of HSI in predicting food quality parameters and safety properties was closely associated with appropriate data mining methods, the prediction models were established based upon one linear algorithm (PLSR) and two non-linear algorithms (BP-NN and LS-SVM) using the three wavelet features. Table 1 lists their corresponding performance. Among the three wavelet feature sets, the performance of non-linear regression models were better than that of linear regression models. The possible reason might be that the wavelet transformation is a type of non-linear decomposition and the extracted wavelet features cannot be handled properly by linear regression algorithms such as PLSR (Heijmans & Goutsias, 2000). Satisfactory predicting accuracies ($R_p^2 > 0.90$, RMSEP < 2.04 and RPD > 2.79) were obtained from non-linear calibration models based on all three wavelet features, which demonstrated that wavelet features were sufficient to establish a robust and accurate model for predicting the TVB-N contents of prawns during the cold storage. By checking the performance of three algorithms, LS-SVM was considered as the most suitable regression algorithm for building prediction models. In order to avoid the negative effect resulting from the unsuitable regression algorithm (PLSR), only the performances of LS-SVM

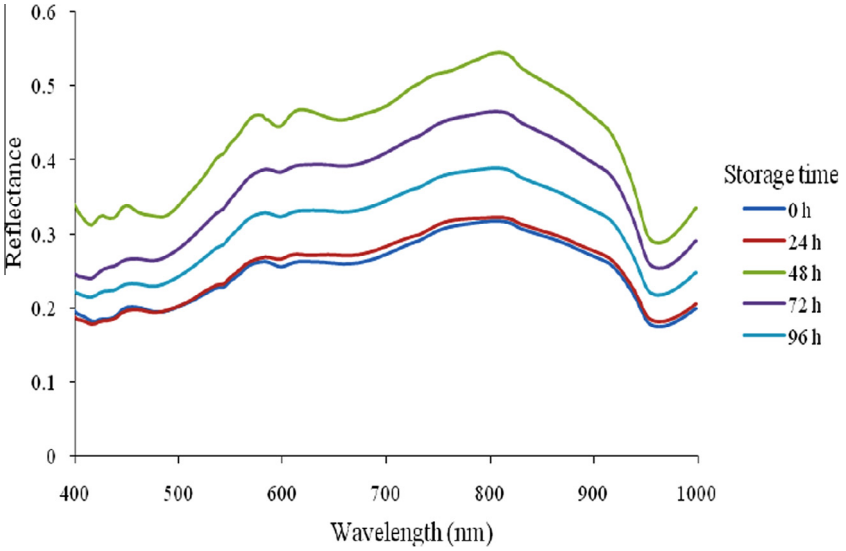

Fig. 4. Average spectra features of the tested prawns at different cold storage periods.

Table 1
Performance of four models for predicting TVB-N contents of prawns based on wavelet features.

Wavelet features	Calibration model	Variable number	Calibration		Prediction		
			R_c^2	RMSEC	R_p^2	RMSEP	RPD
Energy	PLSR	8	0.401	4.102	0.321	6.365	0.943
	LS-SVM	8	0.952	1.184	0.928	1.136	3.655
	BP-NN	8	0.942	1.298	0.901	2.036	2.799
Entropy	PLSR	8	0.164	4.847	0.133	4.986	0.864
	LS-SVM	8	0.997	0.279	0.950	0.874	4.395
	BP-NN	8	0.987	0.875	0.921	1.098	4.063
Modulus maxima	PLSR	20	0.342	4.163	0.238	4.416	0.975
	LS-SVM	20	0.998	0.256	0.955	0.712	4.799
	BP-NN	20	0.975	0.946	0.932	1.159	4.165

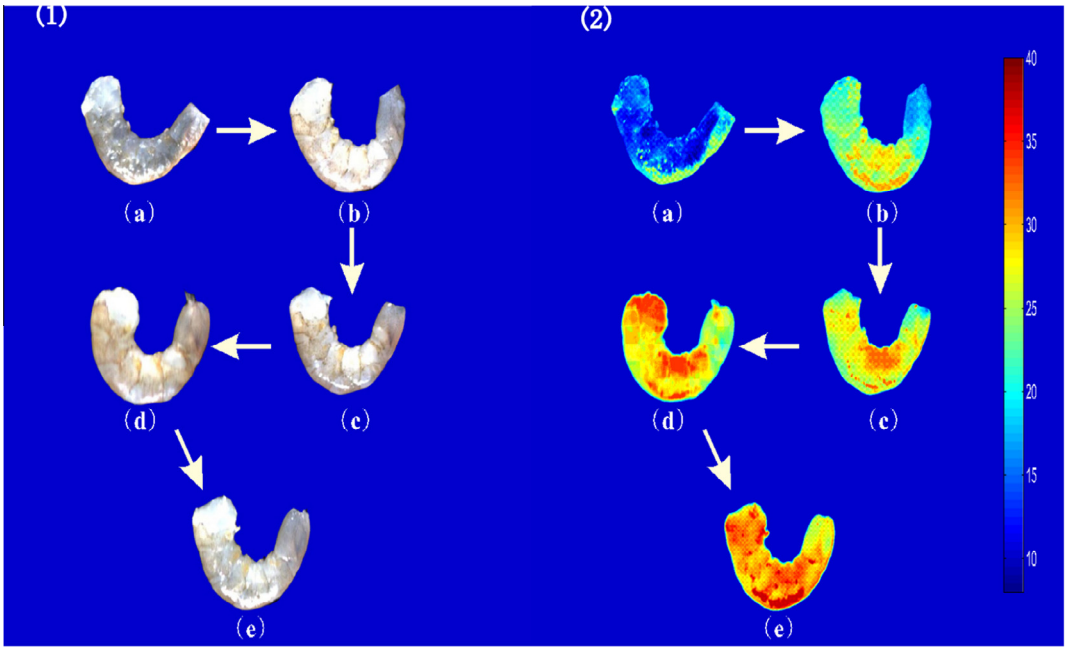

Fig. 5. Examples of oranginal hyperspectral images (1) and TVB-N distribution maps (2) of prawns. (a), (b), (c), (d) and (e) represent the storage period of 0 h, 24 h, 48 h, 72 h and 96 h, respectively.

and BP-NN model were considered to find the best wavelet features for quantification analysis. The modulus maxima showed a better performance than the other two features both in LS-SVM and BP-NN models for predicting TVB-N contents in prawns, possibly because modulus maxima not only calculates the variations of signal value (spectrum) but also contains the information of structure and shape of signal (spectrum) (Tu, Hwang, & Ho, 2005). With a high prediction accuracy of $R_p^2 = 0.9547$, RMSEP = 0.7213 and RPD = 4.799, the LS-SVM model based on modulus maxima features was regarded as the best model for determining the TVB-N contents in prawns during cold storage. This result demonstrated considerable progress compared with Cheng et al. (2013) who used traditional spectral features for investigating the effects of frozen storage on the TVB-N contents of grass carp fillets.

3.5. Visualization of TVB-N distribution of prawn samples

The implementation of a visualization process would be helpful to understand the variation of TVB-N contents within prawn muscles during cold storage, which is impossible to observe visually. In this study, the optimized model based on UVE-LS-SVM using modulus maxima features was used for visualizing the TVB-N distribution maps of prawn samples by transferring the model to each pixel of the image to predict TVB-N contents in all spots of prawns. Fig. 5 shows examples of original hyperspectral images (1) and visualization of TVB-N distribution map (2) of prawns at five different cold storage periods. Obviously, it is hard to tell the difference levels of TVB-N distribution of prawn samples from the captured hyperspectral images in Fig. 5(1) directly. As shown in Fig. 5(2), high TVB-N values were shown in red color while the low values were in blue color. As the storage time increased, the distribution maps exhibited an increase in overall TVB-N contents from blue to red, a clear indication of spoilage uptake during the cold storage of prawns. Although it is difficult to visually observe the difference in TVB-N contents from location to location, the difference could be easily discerned from the final distribution maps. The density and intensity of TVB-N contents of the head and back locations were clearly higher than those of other locations, which might be subjected to the high concentration of microorganisms in prawns in those locations before cold storage.

The concentration maps demonstrated that HSI was a promising and useful tool for predicting and visualizing TVB-N contents of prawns at different cold storage periods. With such TVB-N contents distribution map, it was helpful and meaningful to evaluate the accumulation of TVB-N contents in prawns during cold storage.

More importantly, the distribution map could well facilitate process monitoring and freshness quality control in the industry, and provide information for the right consumption of prawn products with correct label, classification and price.

4. Conclusions

The potential for predicting TVB-N contents using a Vis–NIR (400–1000 nm) HSI system in combination with wavelet features were investigated in this study. The accuracies of the three wavelet features (energy, entropy, modulus maxima) demonstrated that the information obtained was sufficient to evaluate TVB-N variation in prawns during cold storage. The non-linear regression methods (LS-SVM and BP-NN) were more suitable to deal with wavelet features than linear regression method (PLSR). The UVE-LS-SVM model using the modulus maxima features was considered as the best model for the determination of TVB-N contents, which showed high prediction ability with $R_p^2 = 0.9547$, RMSEP = 0.7213 and RPD = 4.799. Additionally, visualization maps of TVB-N distribution were created using UVE-LS-SVM model for further understanding and better monitoring the loss of prawn freshness during cold storage. The current results showed that this VIS–NIR HSI technique coupled with wavelet analysis was an effective and powerful tool for rapid and non-destructive determination and assessment of prawn freshness.

Acknowledgements

The authors gratefully acknowledge the financial support from Guangdong Province Government (China) through the program of "Leading Talent of Guangdong Province (Da-Wen Sun)". This research was also supported by the National Key Technologies R&D Program (2014BAD08B09), the Natural Science Foundation of Guangdong Province (2014A030313244), the International S&T Cooperation Programme of China (2015DFA71150), the International S&T Cooperation Projects of Guangdong Province (2013B051000010) and the Key Projects of Administration of Ocean and Fisheries of Guangdong Province (A201401C04). Especial thanks to Dr Dan Liu from South China University of Technology for her kind suggestions.

References

Abramovich, F., Bailey, T. C., & Sapatinas, T. (2000). Wavelet analysis and its statistical applications. *Journal of the Royal Statistical Society: Series D (The Statistician), 49*(1), 1–29.

Alasalvar, C., Taylor, K. D. A., Öksüz, A., Garthwaite, T., Alexis, M. N., & Grigorakis, K. (2001). Freshness assessment of cultured sea bream (*Sparus aurata*) by chemical, physical and sensory methods. *Food Chemistry, 72*(1), 33–40.

Allen, R. L., & Mills, D. (2004). *Signal analysis: time, frequency, scale, and structure*. New York, USA: Wiley, p. 25–54.

Arvanitoyannis, I. S., & Stratakos, A. C. (2012). Application of modified atmosphere packaging and active/smart technologies to red meat and poultry: a review. *Food and Bioprocess Technology, 5*(5), 1423–1446.

Barbin, D. F., ElMasry, G., Sun, D.-W., & Allen, P. (2012a). Predicting quality and sensory attributes of pork using near-infrared hyperspectral imaging. *Analytica Chimica Acta, 719*, 30–42.

Barbin, D., ElMasry, G., Sun, D.-W., & Allen, P. (2012b). Near-infrared hyperspectral imaging for grading and classification of pork. *Meat Science, 90*(1), 259–268.

Barclay, V. J., Bonner, R. F., & Hamilton, I. P. (1997). Application of wavelet transforms to experimental spectra: smoothing, de-noising, and data set compression. *Analytical Chemistry, 69*, 78–90.

Barlocco, N., Vadell, A., Ballesteros, F., Galietta, G., & Cozzolin, D. (2006). Predicting intramuscular fat, moisture and Warner-Bratzler shear force in pork muscle using NIR spectroscopy. *Animal Science, 83*, 111–116.

Boashash, B. (1991). *Time-frequency signal analysis in advances in spectrum analysis and array processing, Vol. 1*. NJ: Prentice-Hall, pp. 433-444.

Cai, J., Chen, Q., Wan, X., & Zhao, J. (2011). Determination of total volatile basic nitrogen (TVB-N) content and Warner-Bratzler shear force (WBSF) in pork using Fourier transform near infrared (FT-NIR) spectroscopy. *Food Chemistry, 126*(3), 1354–1360.

Castro, P., Padrón, J. C. P., Cansino, M. J. C., Velázquez, E. S., & Larriva, R. M. D. (2006). Total volatile base nitrogen and its use to assess freshness in European sea bass stored in ice. *Food Control, 17*(4), 245–248.

Centner, V., Massart, D. L., Noord, O., Jong, S., Vandeginste, B. M., & Sterna, C. (1996). Elimination of uninformative variables for multivariate calibration. *Analytical Chemistry, 68*, 3851–3858.

Chen, G. Y., Zhu, W. P., & Xie, W. F. (2012). Wavelet-based image denoising using three scales of dependency. *IET Imaging Processing, 6*(6), 756–760.

Cheng, J. H., Sun, D.-W., Zeng, X. A., & Pu, H. B. (2014). Non-destructive and rapid determination of TVB-N content for freshness evaluation of grass carp (*Ctenopharyngodon idella*) by hyperspectral imaging. *Innovative Food Science and Emerging Technologies, 21*, 179–181.

Cho, D., Bui, T. D., & Chen, G. Y. (2009). Image denoising based on wavelet shrinkage using neighbor and level dependency. *International Journal of Wavelets, Multiresolution and Information Processing, 7*(3), 299–311.

Costa, C., Antonucci, F., Pallottino, F., Aguzzi, J., Sun, D.-W., & Menesatti, P. (2011). Shape analysis of agricultural products: a review of recent research advances and potential application to computer vision. *Food and Bioprocess Technology, 4*(5), 673–692.

Cui, Z.-W., Sun, L.-J., Chen, W., & Sun, D.-W. (2008). Preparation of dry honey by microwave-vacuum drying. *Journal of Food Engineering, 84*(4), 582–590.

Dai, Q., Cheng, J. H., Sun, D.-W., & Zeng, X. A. (2014). Potential of hyperspectral imaging for non-invasive determination of mechanical properties of prawn (*Metapenaeus ensis*). *Journal of Food Engineering, 136*, 64–72.

Delgado, A. E., & Sun, D.-W. (2002). Desorption isotherms and glass transition temperature for chicken meat. *Journal of Food Engineering, 55*(1), 1–8.

Donoho, D. L. (1995). Denoising by soft-thresholding. *IEEE Transactions on Information Theory, 41*(3), 613–627.

ElMasry, G., Barbin, D. F., Sun, D.-W., & Allen, P. (2012). Meat quality evaluation by hyperspectral imaging technique: an overview. *Critical Reviews in Food Science and Nutrition, 52*(8), 689–711.

ElMasry, G., Kamruzzaman, M., Sun, D.-W., & Allen, P. (2012). Principles and applications of hyperspectral imaging in quality evaluation of agro-food products: a review. *Critical Reviews in Food Science and Nutrition, 52*(11), 999–1023.

Elmasry, G., Sun, D.-W., & Allen, P. (2011). Non-destructive determination of water-holding capacity in fresh beef by using NIR hyperspectral imaging. *Food Research International, 44*(9), 2624–2633.

ElMasry, G., Sun, D.-W., & Allen, P. (2013). Chemical-free assessment and mapping of major constituents in beef using hyperspectral imaging. *Journal of Food Engineering, 117*(2), 235–246.

Feng, Y. Z., & Sun, D.-W. (2012). Application of hyperspectral imaging in food safety inspection and control: a review. *Critical Reviews in Food Science and Nutrition, 52*(11), 1039–1058.

Grafakos, L. (2008). *Classical and modern Fourier analysis, Vol. 1*. Prentice-Hall, pp. 126-153.

Gributs, C. E. W., & Burns, D. H. (2006). Parsimonious calibration models for near-infrared spectroscopy using wavelets and scaling functions. *Chemometrics and Intelligent Laboratory Systems, 83*, 44–53.

Guy, F., Prache, S., Thomas, A., Bauchart, D., & Andueza, D. (2011). Prediction of lamb meat fatty acid composition using near-infrared reflectance spectroscopy (NIRS). *Food Chemistry, 127*, 1280–1286.

He, H.-J., Wu, D., & Sun, D.-W. (2013). Non-destructive and rapid analysis of moisture distribution in farmed Atlantic salmon (Salmo salar) fillets using visible and near-infrared hyperspectral imaging. *Innovative Food Science & Emerging Technologies, 18*, 237–245.

Heijmans, H. J., & Goutsias, J. (2000). Nonlinear multiresolution signal decomposition schemes. ii. Morphological wavelets. *Image Processing, IEEE Transactions on, 9*(11), 1897–1913.

Huang, L., Zhao, J., Chen, Q., & Zhang, Y. (2014). Nondestructive measurement of total volatile basic nitrogen (TVB-N) in pork meat by integrating near infrared spectroscopy, computer vision and electronic nose techniques. *Food Chemistry, 145*, 228–236.

Iglesias, J., Medina, I., Bianchi, F., Careri, M., Mangia, A., & Musci, M. (2009). Study of the volatile compounds useful for the characterisation of fresh and frozen-thawed cultured gilthead sea bream fish by solid-phase microextraction gas chromatography–mass spectrometry. *Food Chemistry, 115*(4), 1473–1478.

Jackman, P., Sun, D.-W., Du, C.-J., & Allen, P. (2009). Prediction of beef eating qualities from colour, marbling and wavelet surface texture features using homogenous carcass treatment. *Pattern Recognition, 42*(5), 751–763.

Kamruzzaman, M., ElMasry, G., Sun, D.-W., & Allen, P. (2012). Non-destructive prediction and visualization of chemical composition in lamb meat using NIR hyperspectral imaging and multivariate regression. *Innovative Food Science & Emerging Technologies, 16*, 218–226.

Khojastehnazhand, M., Khoshtaghaza, M. H., Mojaradi, B., Rezaei, M., Goodarzi, M., & Saeys, W. (2014). Comparison of visible-near infrared and short wave infrared hyperspectral imaging for the evaluation of rainbow trout freshness. *Food Research International, 56*, 25–34.

Kiani, H., & Sun, D.-W. (2011). Water crystallization and its importance to freezing of foods: a review. *Trends in Food Science & Technology, 22*(8), 407–426.

Koutsoumanis, K., & Nychas, G. J. E. (2000). Application of a systematic experimental procedure to develop a microbial model for rapid fish shelf life predictions. *International Journal of Food Microbiology, 60*(2), 171–184.

Liu, D., Sun, D. W., & Zeng, X. A. (2014). Recent advances in wavelength selection techniques for hyperspectral image processing in the food industry. *Food and Bioprocess Technology, 7*(2), 307–323.

Lorente, D., Aleixos, N., Gómez-Sanchis, J., Cubero, S., García-Navarrete, O. L., & Blasco, J. (2012). Recent advances and applications of hyperspectral imaging for fruit and vegetable quality assessment. *Food and Bioprocess Technology, 5*(4), 1121–1142.

Mallat, S. G. (1989). A theory for multiresolution signal decomposition: the wavelet representation. *IEEE Transactions on Pattern Analysis and Machine Intelligence, 11*(7), 674–693.

Martinez, I., & Jakobsen Friis, T. (2004). Application of proteome analysis to seafood authentication. *Proteomics, 4*(2), 347–354.

Olafsdottir, G., Martinsdóttir, E., Oehlenschläger, J., Dalgaard, P., Jensen, B., Undeland, I., & Nilsen, H. (1997). Methods to evaluate fish freshness in research and industry. *Trends in Food Science and Technology, 8*(8), 258–265.

Pu, H., Sun, D. W., Ma, J., Liu, D., & Cheng, J. H. (2014). Using Wavelet Textural Features of Visible and Near Infrared Hyperspectral Image to Differentiate Between Fresh and Frozen-Thawed Pork. *Food and Bioprocess Technology, 7*(11), 3088–3099.

Pu, H., Xie, A., Sun, D. W., Kamruzzaman, M., & Ma, J. (2015). Application of wavelet analysis to spectral data for categorization of lamb muscles. *Food and Bioprocess Technology, 8*(1), 1–16.

Reddy, G., & Srikar, L. N. (1991). Preprocessing ice storage effects on functional properties of fish mince protein. *Journal of Food Science, 56*(4), 965–968.

Sun, D.-W., & Eames, I. W. (1996). Performance characteristics of HCFC-123 ejector refrigeration cycles. *International Journal of Energy Research, 20*(10), 871–885.

Sun, D.-W. (2004). Computer vision – An objective, rapid and non-contact quality evaluation tool for the food industry. *Journal of Food Engineering, 61*(1), 1–2.

Talens, P., Mora, L., Morsy, N., Barbin, D. F., ElMasry, G., & Sun, D.-W. (2013). Prediction of water and protein contents and quality classification of Spanish cooked ham using NIR hyperspectral imaging. *Journal of Food Engineering, 117*(3), 272–280.

Tu, C. L., Hwang, W. L., & Ho, J. (2005). Analysis of singularities from modulus maxima of complex wavelets. *Information Theory, IEEE Transactions on, 51*(3), 1049–1062.

Wang, L. J., & Sun, D.-W. (2002a). Modelling vacuum cooling process of cooked meat – part 2: mass and heat transfer of cooked meat under vacuum pressure. *International Journal of Refrigeration-Revue Internationale Du Froid, 25*(7), 862–871.

Wang, H. H., & Sun, D.-W. (2002b). Melting characteristics of cheese: analysis of effect of cheese dimensions using computer vision techniques. *Journal of Food Engineering, 52*(3), 279–284.

Wang, L. J., & Sun, D.-W. (2004). Effect of operating conditions of a vacuum cooler on cooling performance for large cooked meat joints. *Journal of Food Engineering, 61*(2), 231–240.

Wu, D., He, Y., & Feng, S. (2008). Short-wave near-infrared spectroscopy analysis of major compounds in milk powder and wavelength assignment. *Analytica Chimica Acta, 610*(2), 232–242.

Wu, J., Peng, Y., Li, Y., Wang, W., Chen, J., & Dhakal, S. (2012b). Prediction of beef quality attributes using VIS/NIR hyperspectral scattering imaging technique. *Journal of Food Engineering, 109*(2), 267–273.

Wu, D., & Sun, D.-W. (2013). Potential of time series-hyperspectral imaging (TS-HSI) for non-invasive determination of microbial spoilage of salmon flesh. *Talanta, 111*, 39–46.

Wu, D., Sun, D.-W., & He, Y. (2012). Application of long-wave near infrared hyperspectral imaging for measurement of color distribution in salmon fillet. *Innovative Food Science and Emerging Technologies, 16*, 361–372.

Zheng, L. Y., & Sun, D.-W. (2004). Vacuum cooling for the food industry – a review of recent research advances. *Trends in Food Science & Technology, 15*(12), 555–568.

Zhu, F., Zhang, H., Shao, Y., He, Y., & Ngadi, M. (2013). Mapping of fat and moisture distribution in atlantic salmon using near-infrared hyperspectral imaging. *Food and Bioprocess Technology, 7*(4), 1208–1214.